

Fluid Flow Dynamics of blood through the Endothelial Glycocalyx

Aparna Gupta

University of Arizona

MATH 481

Dr. Laura Miller, Dr. Matea Santiago

12/03/2023

Table of Contents

Fluid Flow Dynamics of Blood through the Endothelial Glycocalyx.....	4
Methods	9
3D Model	9
Model Specifications.....	9
Flow Visualization with Dye injection	11
Computational Fluid Dynamics Simulations with Navier-Stokes Equations.....	12
Reynold’s Number	14
Actual Reynold’s Number for true biological conditions	14
Reynold’s Numbers for Experimental Flow Visualization	15
Results	15
Flow Visualization	15
Numerical Simulations.....	16
Primary Simulation Results.....	16
Comparison of Wall-Shear stress	18
Comparison of Pressure experienced by the structure	19
Discussion.....	20
References.....	22

Abstract

This study investigates the fluid flow dynamics of blood through the endothelial glycocalyx, employing physical models and computational simulations using Ansys. The endothelial surface glycocalyx, a crucial component in vascular health, is examined due to its role in various pathological conditions. The study integrates experimental dye visualization and numerical simulations, highlighting the complex nature of blood flow dynamics. In the experimental phase, 3D-printed models of glycocalyx with and without side chains are subjected to flow tank experiments using fluorescein dye injection. The study employs complex models designed in SolidWorks, with side chains creating challenges in meshing. Computational simulations in Ansys focus on glycocalyx models without side chains, exploring the impact of spacing variations on shear stress. The main results reveal discrepancies between dye visualization and CFD simulations, emphasizing the limitations of traditional methods. While dye visualization suggests increased speed with reduced spacing, CFD simulations show a slowdown, aligning with the study's hypothesis. The study validates the hypothesis that tightly packed cylinders slow flow more at low Reynolds numbers. Relating results to broader questions, the study emphasizes the potential of low spacing to shield the endothelial layer from high pressure and shear stress, contributing to the understanding of vascular dynamics. However, limitations such as model scale differences and Reynolds number discrepancies are acknowledged, calling for future experiments with improved design and matching biological conditions. The proposed future work suggests exploring models with side chains, adjusting Reynolds numbers, and utilizing advanced simulation techniques. This comprehensive approach aims to refine understanding and provide more realistic insights into fluid dynamics around cylinders, ultimately contributing to advancements in vascular health research.

Fluid Flow Dynamics of Blood through the Endothelial Glycocalyx

The main aim of this project is to study the blood flow through the vascular endothelial surface layer and glycocalyx protein present on the surface using physical models and computational simulations of fluid dynamics using Ansys. On the inner surface of our blood vessels, there is a thin membrane called the endothelial surface glycocalyx (Figure 1A and 1B) that consists of proteoglycans (hydrophilic molecules, that assist in providing viscoelasticity and turgor to the vasculature and participate in the regulation of vascular permeability, lipid metabolism, hemostasis, and thrombosis), glycosaminoglycans (negatively charged long unbranched side chains present on proteoglycans), and glycoproteins (membrane-bound proteins with small branched carbohydrate side chains).

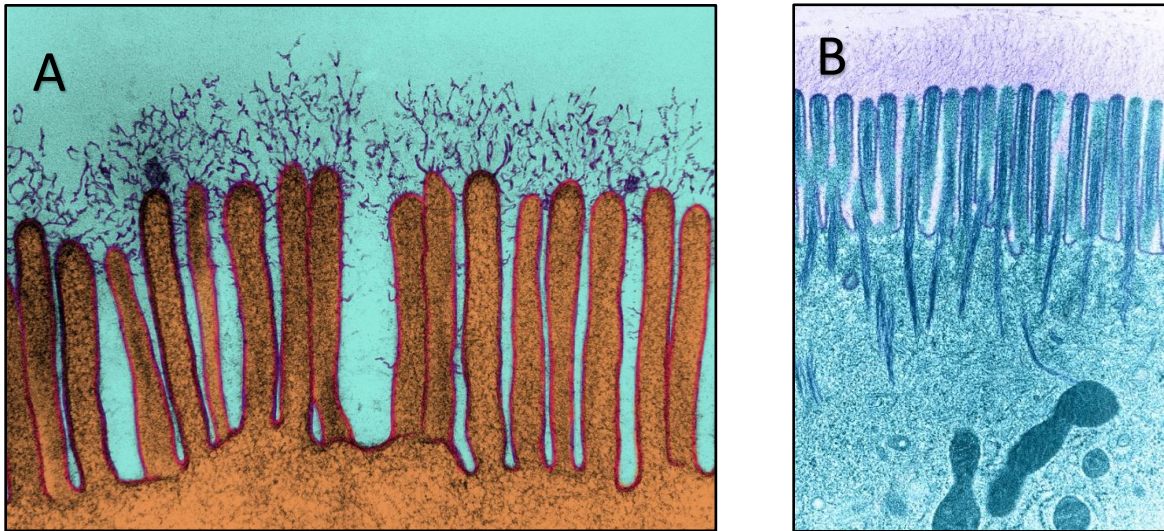
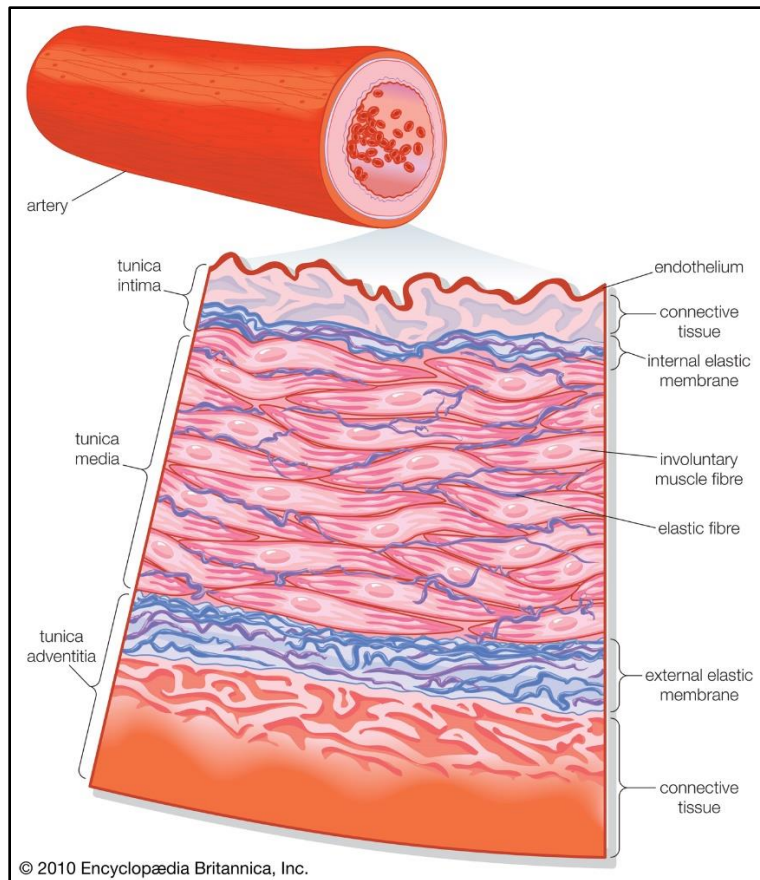


(Figure 1A: Epithelial Glycocalyx with Branching; Figure 1B: glycocalyx present on intestinal epithelium)

The vascular wall is a very complex multilayer structure. The blood vessels are composed of four main layers - general appearance, Tunica Intima, Tunica Media, and Tunica Externa (Figure 2). The Tunica Intima consists of the endothelium layer, below the Tunica Intima, Tunica Media is present that provides support to the vessel and participates in regulating blood flow and pressure, and the Tunica Externa provides tensile strength to the blood vessels. The motivation behind studying the blood flow



dynamics through endothelial surface glycocalyx present on the Tunica Intima is that these structures play a major role in several pathological conditions like cardiovascular diseases, diabetes, kidney disease, sepsis, and trauma. It also has an important role in vascular processes, as it regulates vascular permeability, cellular interactions with the endothelium, mechanical signal transduction, and molecular bioavailability and signaling. The endothelial glycocalyx

(*Figure 2: cross-section of an artery depicting its multiple layers*) may get damaged due to exposure to shear stress and oxidative stress in conditions such as diabetes, sepsis, etcetera. Therefore, studying the flow of blood through the endothelial glycocalyx is essential to understanding how cardiovascular diseases can be detected more efficiently and acted upon more proactively. Understanding the flow rates and shear stresses within the endothelial surface layer is also essential because it directly impacts several vital mechanisms. For instance, fluid flow induces ionic currents within endothelial cells, leading to deformations of transmembrane proteins. Moreover, it plays a significant role in the convection of extracellular molecules, which subsequently signal various biochemical events within the cell. These events include cytoskeletal rearrangements, gene activation, and the release of vasodilators, all of which have far-reaching implications for cardiovascular health and disease.

Considering the pivotal role that endothelial glycocalyx plays in vascular, pathological, and physiological processes, there have been numerous studies that explore the fluid flow dynamic of the blood through the glycocalyx using experimental as well as computational methods. In one such paper,

[9], researchers conducted an analysis of the flow profile within the endothelial surface layer to gain insights into its role in molecular filtration and various biological processes. Their primary objective was to comprehend how fluid moves through porous layers like endothelium, to better understand how mesoscale filtering and protective layers facilitate biological processes across different life forms. Their approach involved both experimental and computational techniques, which they then compared to analytical outcomes by modeling the layer as a homogeneous porous medium with free-flow conditions above it. For the fluid-structure interaction, the researchers adopted the immersed boundary method and utilized the Navier-Stokes equation to describe fluid motion. Numerical results were obtained using the boundary method, with simulations of fluid-structure interaction involving a single cylinder subjected to periodic flow. The researchers varied parameters such as Reynolds number, the number of cylinders, and the spacing between them to investigate fluid flow patterns. In the examined layer, the experimental findings indicate that bulk flow aligns closely with straightforward analytical models. On the other hand, the numerical outcomes reveal that the spatially averaged flow within the layer is accurately characterized by the Brinkman model. Nonetheless, the numerical results also illustrate that the flow exhibits pronounced three-dimensionality, with fluid entering and exiting the layer. These characteristics fall outside the scope of the Brinkman model and could hold notable implications for biologically relevant volume fractions. The findings in this study offer insights into how changes in the density and height of these structures can modify shear stresses and overall flow patterns.

In another study [5], the need for a more nuanced understanding of the endothelial surface layer's role in mechanotransduction is emphasized, as well as the importance of accurate models that consider its dynamic nature. These findings hold implications for various biological and physiological processes, including vascular regulation and cell signaling. The researchers aim to understand the flow rates and shear stresses within the endothelial surface layer, which is crucial for deciphering how flow-induced ionic currents, transmembrane protein deformations, and the convection of extracellular molecules contribute to cell signaling. Previous mathematical models of flow through the endothelial surface layer were built on specific assumptions, including constant hydraulic permeability, constant height, continuity

across the endothelium, and limited extension into the vessel lumen. These models predicted negligible fluid shear stress near endothelial cell membranes. The highlighted paper challenges these assumptions and provides a more comprehensive model. It characterizes the flow through the endothelial surface layer, treating it as clumps of a Brinkman medium immersed in a Newtonian fluid. Parameters such as clump width, spacing, hydraulic permeability, and the fraction of the vessel lumen occupied by the layer are systematically varied. The study employs the two-dimensional Navier–Stokes equations with an additional Brinkman resistance term, solved using a projection method, resulting in a more accurate representation of flow and shear stresses within the layer. The research uncovers multiple transitions in fluid shear stress, where shear stress at the cell membrane shifts from low to high values. These transitions are of particular significance for cell signaling, especially considering that the composition, density, and height of the endothelial surface layer are likely dynamic.

In a recent research paper [8], the investigation conducted employs fluorescent microparticle image velocimetry in venules and cylindrical collagen microchannels lined with endothelial cells, revealing a significant dissonance in the characterization of the endothelial cell glycocalyx. This vital surface layer, with a thickness of $0.52 \pm 0.28 \mu\text{m}$, is considered hydrodynamically pertinent and fundamentally shapes the mechanical and hydrodynamic conditions at the endothelial cell surface when observed in micro vessels in vivo. However, a conspicuous absence of this layer is noted in human umbilical vein endothelial cells ($0.03 \pm 0.04 \mu\text{m}$ thickness) and bovine aortic endothelial cells ($0.02 \pm 0.04 \mu\text{m}$ thickness) when cultured under standard in vitro conditions. An intriguing revelation emerges when an endothelial surface-bound glycosaminoglycan layer is detected, with a thickness of $0.21 \pm 0.27 \mu\text{m}$. This glycosaminoglycan layer, while not a precise replica of the in vivo endothelial glycocalyx, exhibits similar hydrodynamic characteristics. Its presence is contingent on the introduction of hyaluronan and chondroitin sulfate to the cell culture media at hyper physiological concentrations (0.2 mg/mL perfused for 75 minutes). The repercussions of this glycocalyx disparity within standard in vitro models extend broadly across multiple research areas involving endothelial cell monolayers. These areas encompass microvascular permeability, inflammation, mechanotransduction, and atherosclerosis.

Researchers are prompted to reassess their findings considering this revelation, recognizing that the critical role played by endothelial cell surface chemistry in these processes may markedly deviate from the in vivo observations.

In this study, I will determine the fluid flow profile in steady flow using various models of cylinders imitating the structure of glycocalyx by varying the spacing between the cylinders while keeping the radii of the cylinders and the height of the cylinders constant. The flow fields through the models will be numerically solved by finding the solution to the 3D steady Navier Stokes equations. The numerical simulations' results will be compared to the results derived through experimental simulations performed by fluorescent dye visualization of fluid flow through 3D printed models of the endothelial glycocalyx with as well as without side chains. The results will be compared to the results derived through fluid flow analysis in the paper by Leiderman et al. (2007) and Strickland et al. (2017). I hypothesize that the spacing distances being considered for the cylinders will depict significant variations in shear stress experienced by the structure without side chains and radii variations in the model with side chains can drastically affect the fluency of the flow of blood through the structures and would be consistent with the results presented in Leiderman et al. (2007). Specifically, I hypothesize that at a low Reynolds number, the spacing between the cylinders is directly proportional to the flow velocity, that is, as the spacing increases the flow velocity should increase and vice versa, and the spacing between the cylinders is directly proportional to the shear stress experienced by the structure. The main idea behind conducting this experiment is to prove that tight spacing between the glycocalyx and the presence of side chains shelter the endothelial layer from extreme pressure and wall shear stress, and the above-mentioned factors can significantly impact vascular health. A low glycocalyx count compromises this protective barrier, exposing endothelial cells to heightened stress, potentially leading to endothelial dysfunction, increased susceptibility to inflammation, and impaired vascular function. This underscores the crucial role of glycocalyx in maintaining vascular integrity and highlights its relevance in preventing cardiovascular complications and preserving overall circulatory health.

In the following section of the paper, I will outline the experimental and numerical configurations employed for the investigation. Specifically, the experimental phase entails the application of fluorescein dye to visualize flow patterns within 3D printed models of endothelial glycocalyx with and without side chains. The computational analysis utilizes ANSYS Multiphysics to solve the steady Navier-Stokes equations, simulating flow within identical glycocalyx models without side chains. The results section will present findings from flow visualization through glycocalyx models with varied spacing and will compare the results with the flow visualization through the glycocalyx model with side chains. Simulation results from three distinct glycocalyx models will also be included. In the conclusion section, a comparative analysis will be conducted between the study's results and previous research.

Methods

3D Model

Models of cross-sections of glycocalyx with side chains (figure 3A) and without side chains (designed by Dr. Laura Miller, figure 3B) were designed in SolidWorks and were smoothed and meshed using Meshmixer (Autodesk). The models with side chains were very complex and resulted in a very low orthogonal mesh quality due to which the models without the side chains were used for flow simulation in Ansys. The models with side chains were used for flow visualization with dye injection. The results from both simulations were compared to analyze the impact of side chains on the flow of blood through the structure. For computational purposes, the radii were varied in the models with side chains and the spacing was varied in the models without the side chains. The models with side chains were printed in resin and the models without side chains were printed in PVA- white material, and both the models were printed at Catalyst Studios, University of Arizona. The mentioned materials were chosen to facilitate clear visibility of the dye being injected.

Model Specifications

For modeling flow through glycocalyx with side chains, three models were designed with varying radii. The height of the cylinders and the distance between them were constant for all models, where h (height of cylinders) = 0.025 meters and l (distance between cylinders) = 0.13 meters.

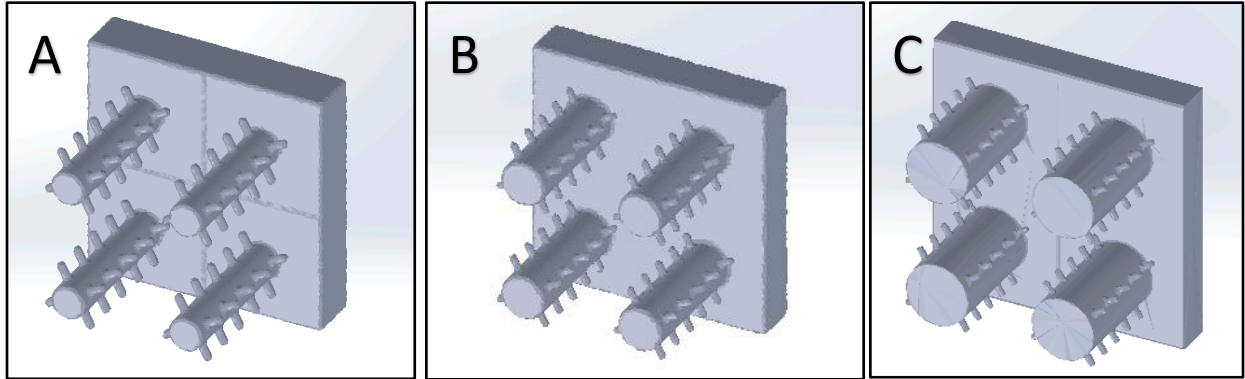


(Figure 3A – Model of glyocalyx with side chains to be 3D printed in resin; A: radius = 0.0025 meters, B: radius = 0.004 meters, C: radius = 0.0065 meters)

For modelling flow through glyocalyx without side chains, three models were printed with varying spacing between them. The height (0.03 meters) and radius of the cylinders were kept constant for all the models. All three models were printed on a base of dimensions 0.15 meters by 0.075 meters. For the loosely packed models, 8 cylinders were placed along the side that is 0.075 meters, and 15 cylinders were placed along the side that is 0.15 meters. For semi-tightly packed model, 10 cylinders were placed along the side that is 0.075 meters and 20 cylinders were placed along the side that is 0.15 meters. For the tightly packed model, 15 cylinders were placed along the side that is 0.075 meters, and 30 cylinders were placed along the side that is 0.15 meters.

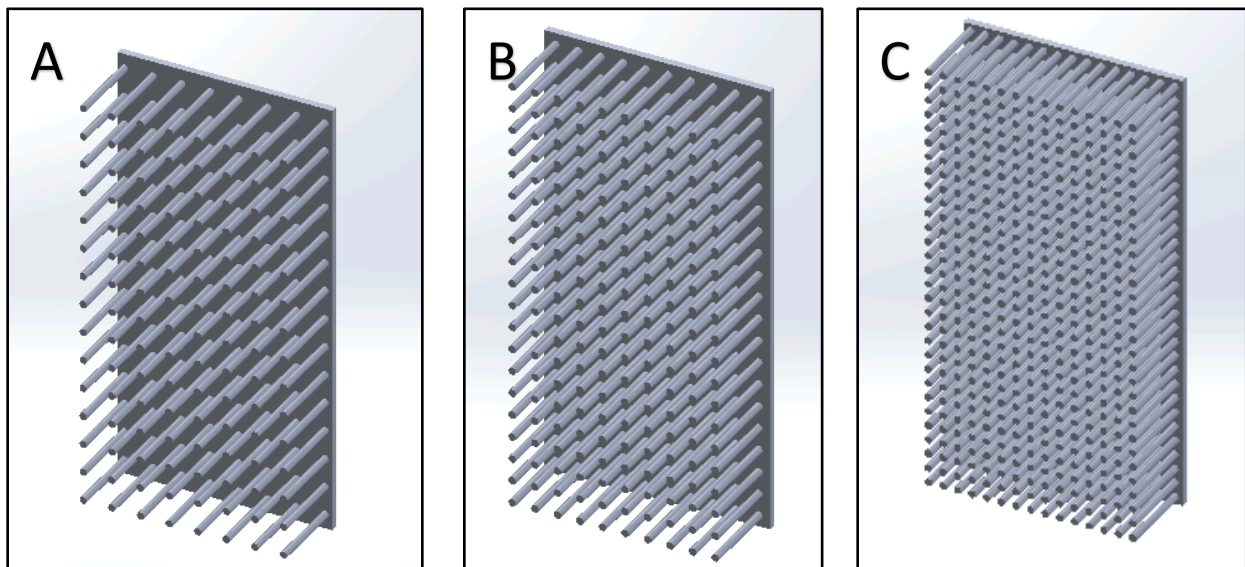


(Figure 3B – Model of glyocalyx without side chains to be 3D printed in PVA-white; A: 8x15 grid, B: 10x20 grid, C: radius = 15x30 grid)

Flow Visualization with Dye Injection

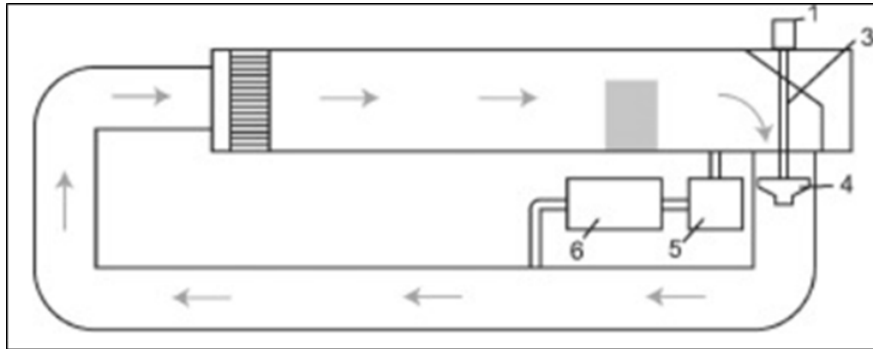


(Figure 4 – 6' x 6' flow tank showing Experimental setup for flow visualization from Vogel and LaBarbera (1978))

The 3D-printed glyocalyx models, both with and without side chains, were positioned within a desktop flow tank featuring a 6' x 6' cross-section and filled with

water to replicate blood flow conditions (Figure 4). To observe the blood flow within the structures, fluorescein dye was introduced. The choice of this dye was based on its heightened visibility, which facilitates easier flow analysis. The dye was carefully pipetted into the structure's inlet and allowed to flow undisturbed, ensuring a clear visualization of the flow path (figure 5).

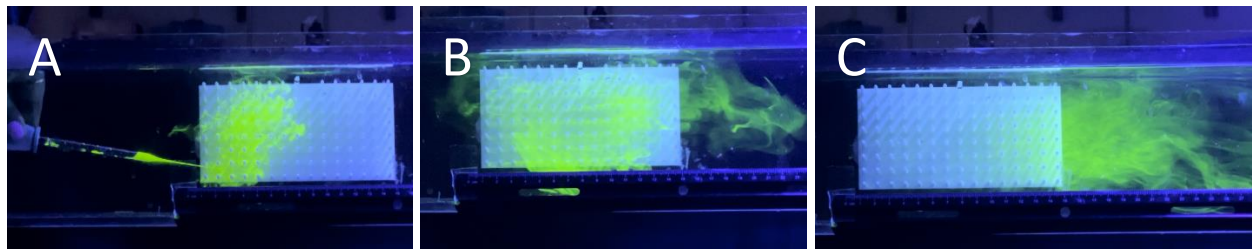


(Figure 5: Sample of Experimental setup and procedure for dye visualization depicting the flow of dye through one of the models without the side chains.)

To ensure optimal visibility, a video was recorded in 3x mode using the cinematic mode on an iPhone 13 Plus. The camera was strategically positioned to center the structures within the frame, especially considering the relatively small size of the side chains and cylinders. Additionally, a black light was positioned directly above the tank to enhance the visibility of the fluorescein dye.

The captured video was analyzed in a meticulous frame-by-frame manner using ImageJ (Rasband, 2018). This analysis aimed to extract quantitative data pertaining to the flow patterns, velocity profiles, and shear stress observed in the experiment. The flow velocity within the model was determined by tracking the time it took for the dye to traverse a predetermined distance, and dividing it by the length of

the structure. The model was 15 cm in length and this length was constant for all three models. Table 1 shows a calculation of these velocities and the relevant time recording. As can be noted, as the spacing decreases the velocity increases in magnitude.

Table 1: Velocity calculation for flow visualization through dye injection				
model	initial time (seconds)	final time (seconds)	measured time (seconds)	velocity (m/s)
loosely packed	5	12	7	0.021
semi-tightly packed	11	17	6	0.025
tightly packed	12	16	4	0.038

Computational Fluid Dynamics Simulations with Navier-Stokes Equations

To gain a deeper understanding of the flow dynamics within the glycocalyx and evaluate key parameters such as wall shear stress, pressure distribution, and velocity profiles, a computational fluid dynamics (CFD) simulation was performed. Three different models with varying space between them, with a constant radius, height of cylinders, and base size, were analyzed. Since the velocity at a given point in space does not vary with time, the simulation involved solving the steady-state form of the Navier-Stokes equations (equation 2), assuming constant temperature, flow rate, and viscosity.

$$\rho(u \cdot \nabla)u = -\nabla p + \mu \nabla^2 \vec{u} + \vec{f}$$

here $\rho \times (u \cdot \nabla)u$ is the acceleration of the fluid parcel, $-\nabla p$ is the pressure gradient (normal forces), $\mu \nabla^2 \vec{u}$ is the viscous term (fluid friction), and \vec{f} is the vector representing the forces acting on the body per unit volume (gravity). In this equation, ρ is the density of the fluid, u is the velocity field, p is the pressure field, and μ is the dynamic viscosity of the fluid.

Utilizing ANSYS Fluent (ANSYS, 2022), laminar flow through the models was numerically simulated. Each of the models had an identical mesh (Figure 6) and an identical size of the domain (Figure 7). The domain boundary defines the extent of the simulated space, influencing the accuracy and relevance of the results. Mesh quality, on the other hand, refers to the discretization of the domain into finite elements or cells. A high-quality mesh is essential for accurate and stable simulations. Well-shaped

elements, proper resolution in critical regions, and smooth transitions between elements contribute to numerical accuracy and convergence. The minimum orthogonal quality of the mesh was lower than 0.001 (Figure 6A) as the model was very complicated and intricate and was deemed to be acceptable considering the time constraints and the limitations of the available hardware.

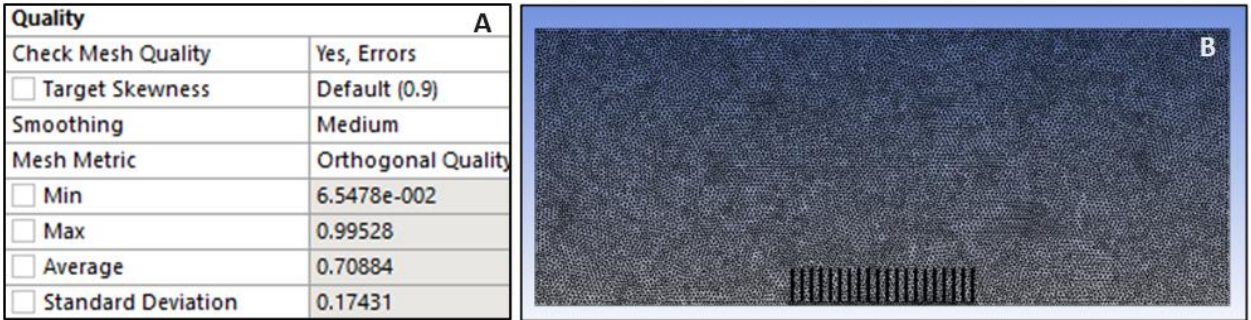
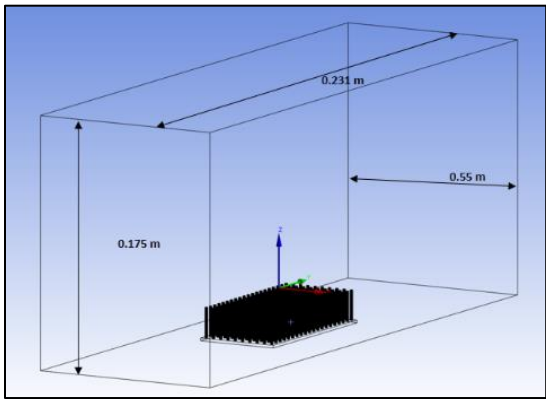


(Figure 6A: Mesh Quality of the model, Figure 6B: Visualization of Mesh)



The length of the model in the x-direction was 0.075 meters, and the domain boundary in that direction was set at 0.2375 meters on either side of the model. The length of the model in the y-direction was 0.15 meters, and the domain boundary in that direction was set at 0.04 meters on either side of the model. The boundary of domain

(Figure 7: boundary conditions of the domain) in the z-direction was set to be 0.175 meters. These values were selected to ensure smooth flow through the model to yield relevant results.

The inlet and outlet were defined at opposite ends of the horizontal axis of the models (Figure 8), and a uniform velocity profile was imposed at the inlet, reflecting the average blood flow velocity through the glycocalyx, set at 0.005 m/s. The simulation ran until convergence was achieved, indicating the attainment of a steady-state solution. Subsequent post-processing was conducted to visualize and analyze the velocity field, pressure distribution, and wall shear stress throughout the glycocalyx. This data offers valuable insights into regions of potential flow disturbance, crucial for comprehending the origins of various cardiovascular diseases. Velocity across the XY plane, keeping the Z-axis variable constant, will be measured and compared for all three models with varying distances.

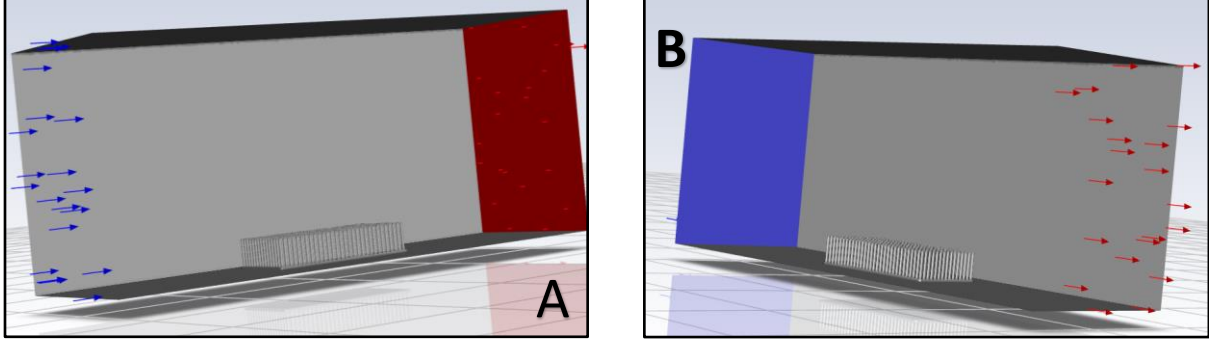


(Figure 8: The computational model of the glyocalyx without the side chains with the inlet direction indicated by the blue arrows and the outlet direction indicated by the red arrows.)

Reynold's Number

Reynolds number associated with the flow of blood through the endothelial glyocalyx was calculated. Reynolds number can be defined as the ratio of inertia force to viscous/friction force. The Reynold number (Re) can be calculated using the following equation,

$$Re = \frac{\rho LU}{\mu} \quad (1)$$

where U represents the characteristic velocity (average velocity within the glyocalyx), μ is the dynamic viscosity of the fluid (blood), L is the characteristic length, and ρ is the density of the fluid (blood).

Actual Reynold's Number for true biological conditions

$$Re = \frac{\rho LU}{\mu} = \frac{1025 \times (1 \times 10^{-6}) \times (1 \times 10^{-3})}{(1 \times 10^{-3})} = 1.15 \times 10^{-3} \quad (2)$$

In this context, L corresponds to the diameter of the vessel, and it is set at 1×10^{-5} m. The characteristic velocity (U) for capillary flow remains constant at 1×10^{-3} m/s. Additionally, the dynamic viscosity of plasma (μ) is specified as 1×10^{-3} Pas, and the density of plasma (ρ) is set at 1025 kg/m^3 (Liederman et. Al., 2017). The Reynolds number, calculated based on these parameters, is confirmed to be less than 2000. This observation leads to the conclusion that the flow can be appropriately characterized as laminar.

Reynold's number for numerical simulations

$$Re = \frac{\rho LU}{\mu} = \frac{1400 \times 0.005 \times 0.001}{15} = 0.467 \times 10^{-2} \quad (3)$$

To get a better understanding of fluid flow patterns, flow through the model was numerically simulated using ANSYS Fluent (ANSYS, 2022). For this experiment, the fluid used for the simulations was corn syrup. This is done to compensate for the fact that the models aren't designed to scale, and hence a denser fluid is used to match the actual Reynolds number. The simulation employed corn syrup as the base fluid, characterized by a density of 1400 kg/m³ and a dynamic viscosity of 15 Pas (Dixon Valve. (2023)). The diameter of the vessel is 0.005 m, and the inlet velocity is 0.001m/s.

Reynold's Numbers for Experimental Flow Visualization

$$Re = \frac{\rho LU}{\mu} = \frac{1000 \times 0.005 \times 0.021}{0.00089} = 117.98 \quad (4)$$

$$Re = \frac{\rho LU}{\mu} = \frac{1000 \times 0.005 \times 0.025}{0.00089} = 140.45 \quad (5)$$

$$Re = \frac{\rho LU}{\mu} = \frac{1000 \times 0.005 \times 0.038}{0.00089} = 213.48 \quad (6)$$

For the experimental fluid analysis through dye injection, the fluid chosen was water with a density of 1000 kg/m³, and a dynamic viscosity of 0.00089 Pas [14]. The diameter of the vessel for all three models, with varying radii, was constant (0.005 m). The inlet velocity, however, was different for each model and has been calculated in Table 1. Reynolds Number was calculated for each model using the inlet velocity calculated in Table 1.

Results

Flow Visualization

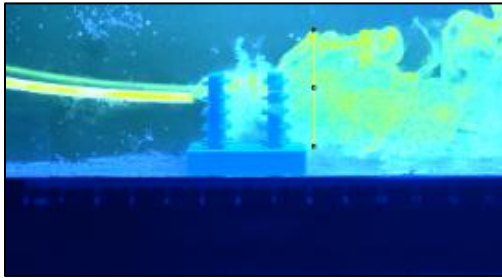


(Figure 9: Measurement of size of wake.)

The wake for the models with side chains and without side chains was calculated using ImageJ (Figure 9), and the results are mentioned in Table 2. It should be noted that at a high Reynold number, the size of the wake increases as the radii size increases. It should also be noted that the size of the wake in each case is longer than the length of the

cylinders, which is 2.25 centimeters.

Table 2: Calculation of Wake	
Models	Size of Wake (cm)
with side chains	
1. $R = 0.0025$ meters	3.496
2. $R = 0.004$ meters	2.661
3. $R = 0.0065$ meters	2.288

Numerical Simulations

The following section presents the results yielded from the Ansys simulations performed on models without the side chains.

Primary Simulation Results

Results from a tightly packed model of glycocalyx without cylinders with an inlet velocity of 0.005 m/s are presented in Figure 10. The spacing between the cylinders is varied with the inlet velocity being the same for each simulation (0.005 m/s). Since we have chosen corn syrup as the fluid, the Re for the simulation is $0.4e-02$. The Reynolds number is an order higher than the actual Reynolds number under physical conditions, as it is difficult to scale the model to the actual size of the structure. The Reynolds number will remain the same for all three variations of the spacing between the cylinders.

A colormap of the magnitude and the direction of the velocity is displayed (10A). The size of the vectors is proportional to the velocity magnitudes. As can be observed, the flow is significantly slower through the structure and the lining of the domain, increasing radially inwards. 3D visualization of streamlines through the structure is displayed next (10B), which displays a linear flow through the structure with most streamlines concentrated at the bottom part of the cylinders. The pressure experienced by the cylinders has been visualized (10C), and it can be observed that the pressure is highest at the inlet and lowest at the outlet, displaying a decreasing pattern through the flow. Figure 10E displays the shear stress exerted by the fluid (Pascals), experienced by the cylinders. The cylinders located at the inlet and outlet positions experience increased shear stress as compared to the cylinders located in the middle cross-section of the structure. Additionally, the top part of all the cylinders experiences a greater wall shear stress compared to the bottom part of the cylinders.

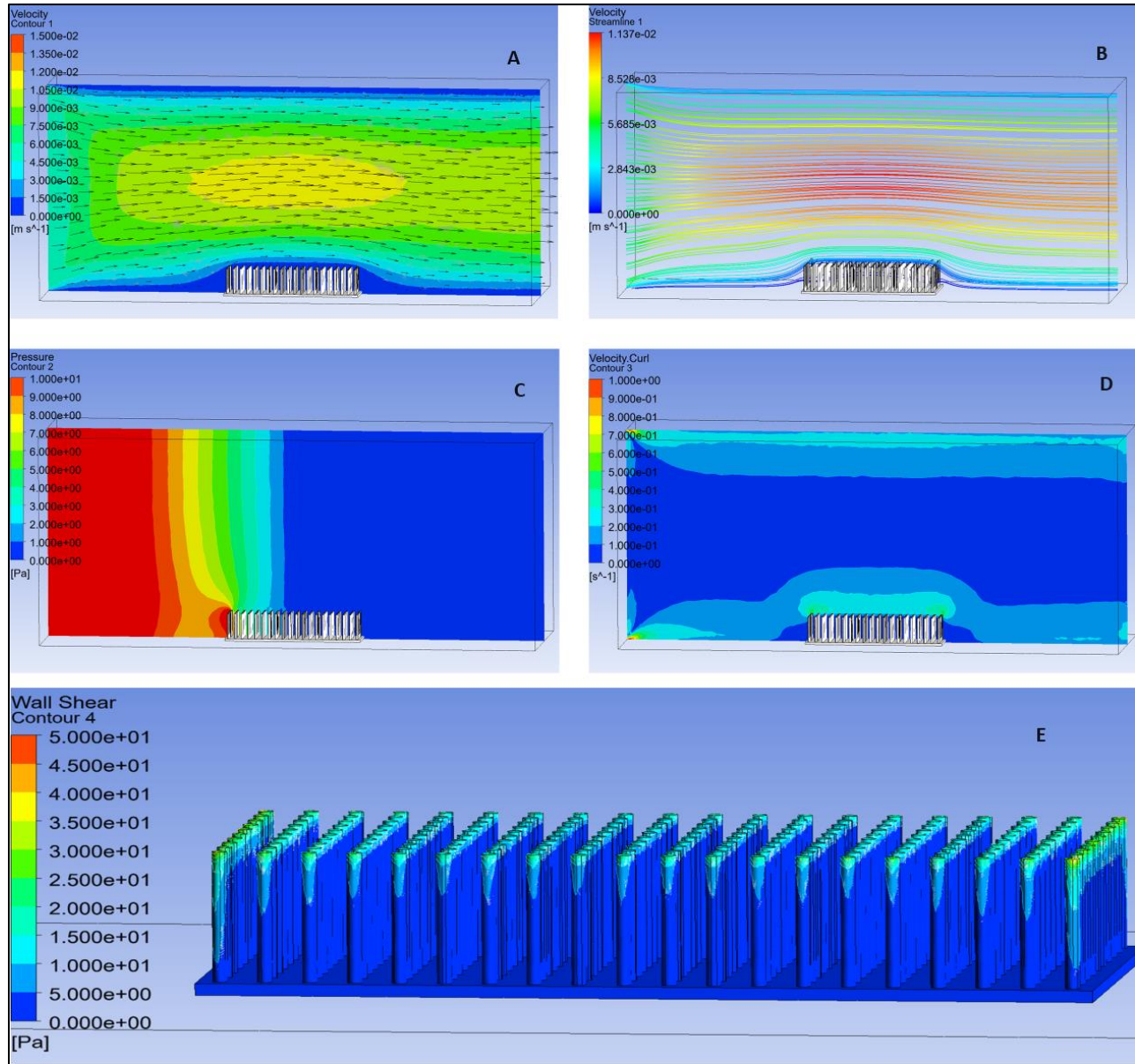


(Figure 10: Simulation results from flow through semi-tightly packed glycocalyx. (A) The figure presents a velocity contour map through the glycocalyx with velocity vectors superimposed, (B) streamline-plot displaying fluid flow through the structure, with the colors representing the magnitude of the velocity, (C) the pressure experienced by the cylinders with the colors representing the magnitude in Pascals, (E) wall shear stress experienced by the cylinders with the color representing the magnitude in Pascals.)

Figure 11 demonstrates the velocity of the fluid along the XY plane of the structure of the glycocalyx model. The z-axis level is constant, and the inlet and outlet are defined at either edge of the glycocalyx structure. The visualization demonstrates that at the point of inlet, the velocity is widely spread across a range of 0 m/s to 6m/s and as the fluid flows through the structure the velocity slows

down and converges to a range of 0 m/s to 2 m/s. It must be noted that this result is valid for a low Reynolds number and is not consistent with the results derived from the dye injection experiment.

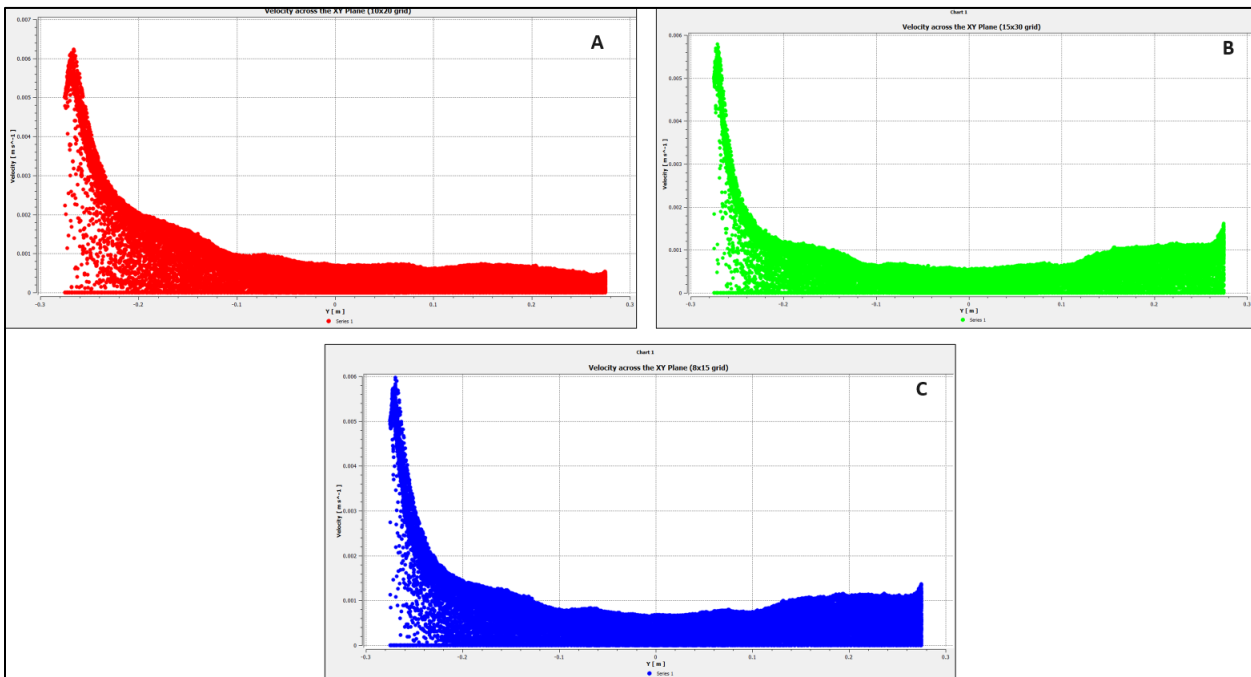


(Figure 11: Velocity along the XY plane through the model)

Comparison of Wall-Shear stress

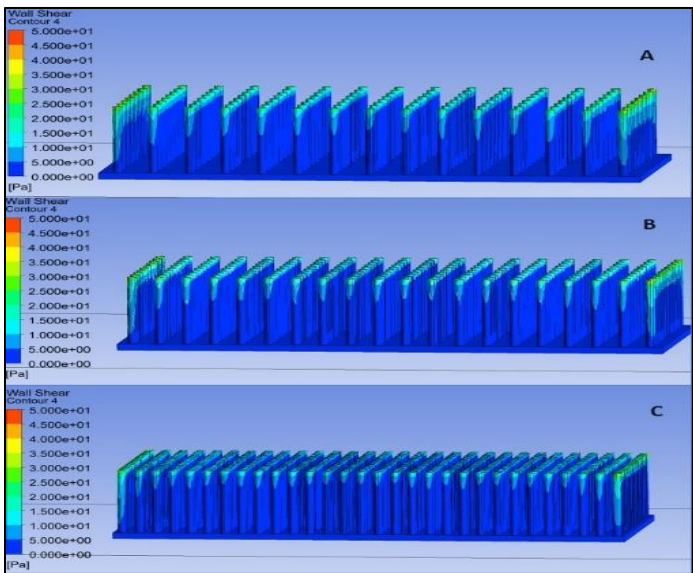


(Figure 12: Wall shear stress visualization)

Figure 12 displays wall shear stress experienced by the three different models, loosely packed, semi-tightly packed, and tightly packed. In all cases, the wall shear stress is the highest at the inlet and outlet points, however as the density of the cylinders increases the wall shear stress experienced by the cylinders decreases as we move down the vertical length of the cylinders.

Comparison of Pressure experienced by the structure

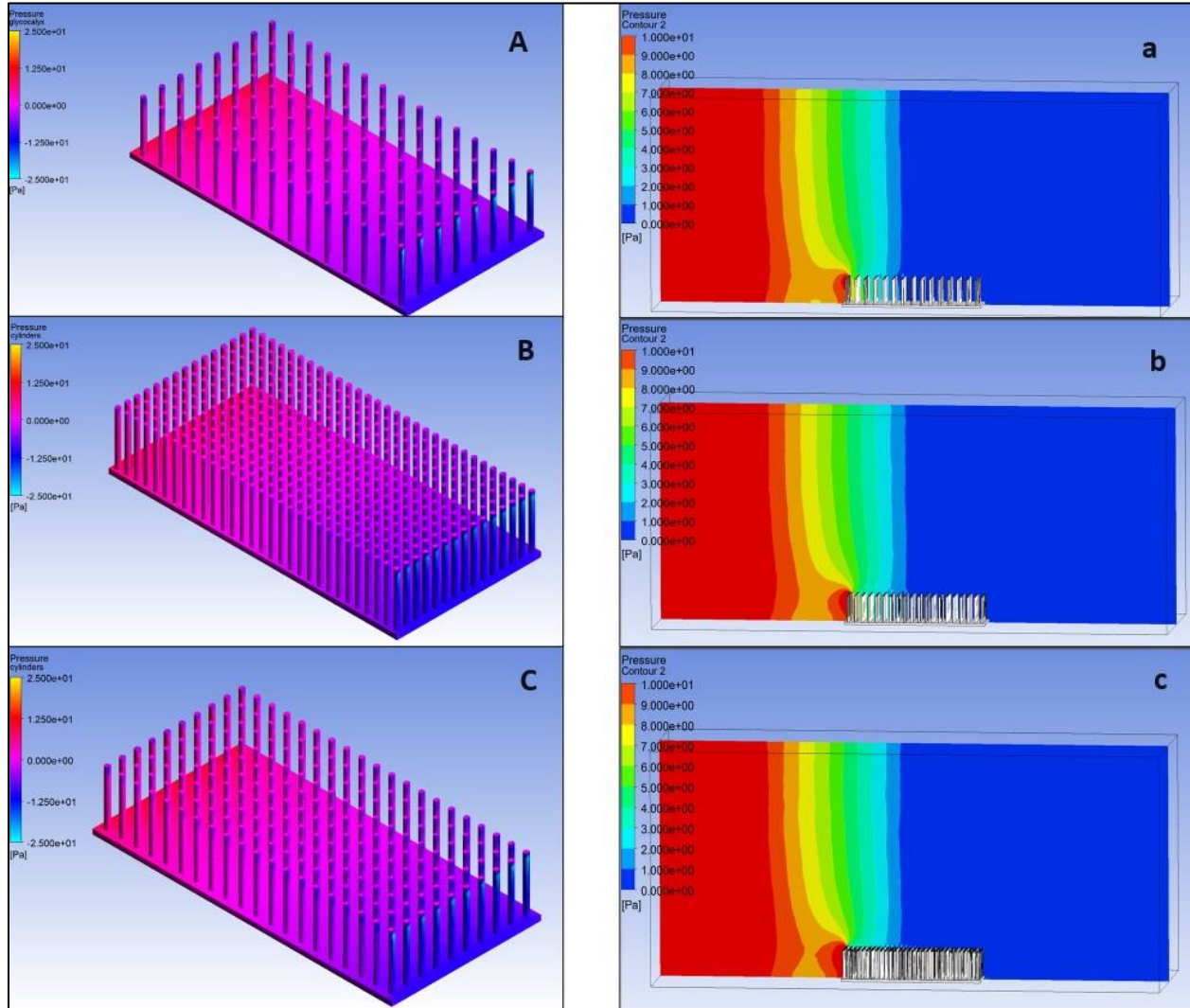


(Figure 13: Pressure visualization across three different models.)

The pressure experienced by the cylinders, in all three models with varying distance between them, as the corn syrup flows through the structure has been visualized in Figure 13. It can be noted that the pressure is higher at the tip of the glycolyx and slightly decreases as we go down the vertical length of the structure. It should also be observed that pressure is higher at the inlet location of the fluid and decreases as the fluid flows through the structure.

Discussion

The interpretation of dye visualization results reveals intriguing aspects of fluid dynamics around cylinders. At a high Reynolds number, the flow accelerates as the spacing reduces, following the principle of mass conservation. Simultaneously, the wake decreases in size with increasing spacing, yet remains longer than the cylinder length in all conditions. Contrastingly, CFD simulations at a low Reynolds number show a slowdown in flow as spacing reduces, aligning more closely with real-life scenarios. At this lower Reynolds number, the wake is almost non-existent, indicating uniform and smooth fluid movement through the structure.

Comparing experimental and CFD results, a notable discrepancy emerges. While dye visualization suggests increased speed with reduced spacing, CFD simulations demonstrate a slowdown. This discrepancy emphasizes the limitations of traditional visualization methods in capturing nuanced fluid behaviors, highlighting the superiority of CFD in modeling complex flow scenarios.

Relating results to the hypothesis, the study emphasizes the significant impact of spacing on shear stress and its potential influence on blood flow fluency. Ansys simulations without side chains show a decrease in wall shear stress with reduced spacing, particularly at the tip of densely packed cylinders. The inverse proportionality between glycocalyx radii and shear stress aligns with expectations. However, challenges in running simulations for models with chains and varying radii underscore the need for future experiments to explore these complexities.

At low Reynolds numbers, tightly packed cylinders indeed slow the flow more, validating a key aspect of the hypothesis. The unverified hypothesis regarding the impact of side chains on flow velocity highlights the study's time limitations and the intricate nature of the model. This underscores the necessity for future work to delve into these complexities and further validate hypotheses.

Relating results to larger questions and motivations, the study posits that a low spacing distance between cylinders can shield the endothelial layer from high pressure and wall shear stress, potentially preventing endothelial dysfunction and associated vascular complications. This insight contributes to the broader understanding of vascular dynamics and motivates further research into preventive measures for

vascular health. These results also align with findings from Leiderman et al. (2007) and Strickland et al. (2017).

Discussing limitations, the study acknowledges issues with model scale, mesh complexity, and the inadequate size of the model with side chains for meaningful results. These challenges underscore the need for improvements in experimental design to enhance accuracy and applicability. Additionally, the difference in Reynolds number highlights the importance of selecting fluids that match biological conditions, a consideration for future studies aiming for more realistic simulations.

Proposed future work includes addressing limitations by exploring models with side chains and varying radii, potentially employing advanced simulation techniques. Adjusting the Reynolds number to match biological conditions is also suggested, emphasizing the need for more accurate representations of real-life scenarios in future experiments. This comprehensive approach aims to refine the understanding of fluid dynamics around cylinders and their implications for vascular health.

References

1. Cerezo-Magaña, M., Bång-Rudenstam, A., & Belting, M. (2023, January 1). *Proteoglycans: A common portal for SARS-COV-2 and extracellular vesicle uptake*. American journal of physiology. Cell physiology. <https://www.ncbi.nlm.nih.gov/pmc/articles/PMC9799137/>
2. Fan, J., Sun, Y., Xia, Y., Tarbell, J. M., & Fu, B. M. (2019). Endothelial surface glycocalyx (ESG) components and ultra-structure revealed by Stochastic Optical Reconstruction Microscopy (STORM). *Biorheology*, 56(2–3), 77–88. <https://doi.org/10.3233/bir-180204>
3. Jin, J., Fang, F., Gao, W., Chen, H., Wen, J., Wen, X., & Chen, J. (2021, September 17). *The structure and function of the glycocalyx and its connection with blood-brain barrier*. Frontiers. <https://www.frontiersin.org/articles/10.3389/fncel.2021.739699/full#:~:text=Research%20has%20proved%20that%20glycocalyx%20can%20maintain%20the,Levy%2C%202019%3B%20Nikmanesh%20et%20al.%2C%202019%3B%20Zuurbier%2C%202019%29>.
4. Lepedda, A. J., Nieddu, G., Formato, M., Baker, M. B., Fernández-Pérez, J., & Moroni, L. (2021, May 3). *Glycosaminoglycans: From vascular physiology to tissue engineering applications*. Frontiers. <https://www.frontiersin.org/articles/10.3389/fchem.2021.680836/full#:~:text=In%20this%20respect%2C%20surface%20functionalization%20with%20drugs%20or,events%2C%20enhancing%20endothelialization%2C%20and%20further%20promoting%20cell%20proliferation>.
5. Leiderman, K. M., Miller, L. A., & Fogelson, A. L. (2008). The effects of spatial inhomogeneities on flow through the endothelial surface layer. *Journal of Theoretical Biology*, 252(2), 313–325. <https://doi.org/10.1016/j.jtbi.2008.01.013>
6. Libretexts. (2021, May 18). 18.2: *Structure and function of blood vessels*. Medicine LibreTexts. [https://med.libretexts.org/Bookshelves/Anatomy_and_Physiology/Human_Anatomy_\(OERI\)/18%3A_A_Cardiovascular_System_Blood_Vessels_and_Circulation/18.02%3A_Structure_and_Function_of_Blood_Vessels](https://med.libretexts.org/Bookshelves/Anatomy_and_Physiology/Human_Anatomy_(OERI)/18%3A_A_Cardiovascular_System_Blood_Vessels_and_Circulation/18.02%3A_Structure_and_Function_of_Blood_Vessels)
7. Moore, K. H., Murphy, H. A., & George, E. M. (2021). The Glycocalyx: A central regulator of vascular function. *American Journal of Physiology-Regulatory, Integrative and Comparative Physiology*, 320(4). <https://doi.org/10.1152/ajpregu.00340.2020>
8. Potter, D. R., & Damiano, E. R. (2008). The hydrodynamically relevant endothelial cell glycocalyx observed in vivo is absent in vitro. *Circulation Research*, 102(7), 770–776. <https://doi.org/10.1161/circresaha.107.160226>
9. Strickland, C., Miller, L., Santhanakrishnan, A., Hamlet, C., Battista, N., & Pasour, V. (2017). Three-dimensional low Reynolds number flows near biological filtering and protective layers. *Fluids*, 2(4), 62. <https://doi.org/10.3390/fluids2040062>
10. Yilmaz, O., Afsar, B., Ortiz, A., & Kanbay, M. (2019, April 23). *The role of endothelial glycocalyx in Health and Disease*. Clinical kidney journal. <https://www.ncbi.nlm.nih.gov/pmc/articles/PMC6768294/>
11. Rasband, W.S. (1997-2018). *ImageJ [Software]*. U. S. National Institutes of Health, Bethesda, Maryland, USA. Imagej. (n.d.). <https://imagej.net/ij/>

12. Viscosity chart - Dixon valve. (n.d.).
<https://dixonvalve.com/sites/default/files/product/files/brochures-literature/viscosity%20chart.pdf>
13. Vogel, S., & LaBarbera, M. (1978). Simple flow tanks for research and teaching. *BioScience*, 28(10), 638–643. <https://doi.org/10.2307/1307394>
14. *Water - dynamic (absolute) and kinematic viscosity vs. temperature and pressure*. Engineering ToolBox. (n.d.). https://www.engineeringtoolbox.com/water-dynamic-kinematic-viscosity-d_596.html